

Application of the triple-deck theory of viscous–inviscid interaction to bodies of revolution

By MING-KE HUANG† AND G. R. INGER

Department of Aerospace Engineering Sciences, University of Colorado,
Boulder, Colorado 80309

Corrigendum 164 pp 502–503

(Received 12 April 1982 and in revised form 15 October 1982)

The general triple-deck theory of laminar viscous–inviscid interaction is extended to axisymmetric bodies. With body radius/length ratios scaled in terms of Reynolds number as $Re^{-\frac{1}{3}\beta}$ ($\beta > 0$), it is found that for $\beta < 3$ the only three-dimensional effect is that on the incoming undisturbed boundary-layer profile as accounted for by the Mangler transformation. When $\beta = 3$, however, an explicit axisymmetric effect on the interaction equations also enters: the upper-deck flow is governed by the equation of axisymmetric potential disturbance flow, whereas the middle and lower decks are still governed by equations of two-dimensional form. When $\beta > 3$, the body is so slender that transverse curvature effects become important and the lower decks too are explicitly influenced by three-dimensional effects. A detailed example application of this theory is given for weak interactions on a flared cylinder and cone in supersonic flow with $\beta \leq 3$. The three-dimensional effects on the interactive pressure and shear-stress distributions are shown to relieve the strength of the interaction and reduce its upstream influence, as expected. Correspondingly, it is found that the smallest flow deflection angle provoking incipient separation increases with increasing axisymmetric body slenderness. These results are shown to be in qualitative agreement with several experimental studies.

1. Introduction

Lighthill (1953), in his classic study of the upstream propagation of small disturbances in shock-wave boundary-layer interactions, first proposed that the interaction region consists of three physically distinct layers or decks: the upper region outside the boundary layer where inviscid potential flow dominates, the main layer which occupies the major part of the boundary layer and behaves as an inviscid rotational flow, and an inner deck where the viscous-disturbance shear stress must be taken into account. Many interaction problems in which the flow properties have a rapid streamwise change, such as the flow around a corner (Lighthill 1953; Stewartson 1971) and the flow past a small hump (Smith 1973), can be treated in this way. A systematic asymptotic study of this triple-deck structure has been given by Stewartson & Williams (1969), Stewartson (1974), Messiter (1970) and Neiland (1969), each of whom independently showed that the resulting problem reduces to solving the usual boundary-layer equations with unusual boundary conditions. Since then, many investigators (Jenson, Burggraf & Rizzetta 1975; Davis & Werle 1976; Williams 1975) have devoted attention to solving these nonlinear equations by numerical methods, and the triple-deck theory has become a powerful tool in the study of viscous–inviscid interaction problems. On the other hand, non-asymptotic

† Permanent address: Department of Aerodynamics, Nanjing Aeronautical Institute, China.

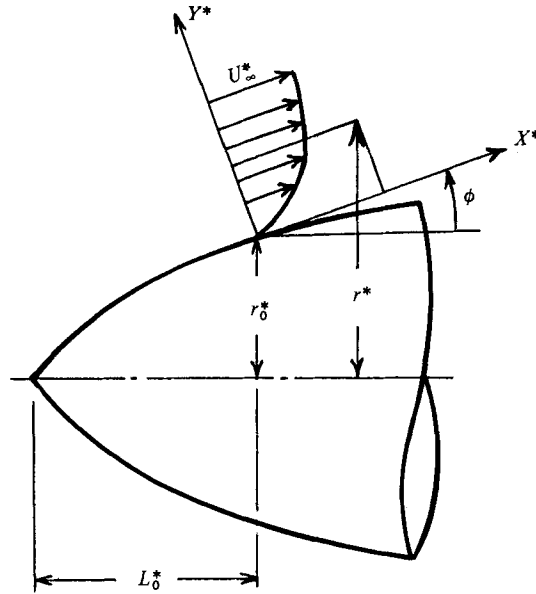


FIGURE 1. Coordinate system on a body of revolution.

versions of this theory have also been developed by Tu & Weinbaum (1976) and by Inger (1980) for laminar and turbulent flows respectively, because the asymptotic theory holds only for extremely large Reynolds number, especially in transonic flow problems.

However, most of the studies to date are only concerned with two-dimensional flow. Those studies published to date that have considered three-dimensional effects (Smith, Sykes & Brighton 1977; Duck 1981; Ryzhov 1980) involve hump-like geometries on otherwise planar surfaces but have not dealt with axisymmetric flow situations. Accordingly, this paper is addressed to a study of viscous-inviscid interaction triple-deck theory for axisymmetric bodies with a detailed illustrative application to the specific problem of a supersonic compressive interaction in a flared body. Section 2 presents a discussion of the general theory for either subsonic or supersonic interactions; the specific supersonic flare problem including an analytical solution for weak compressions is then given and discussed in §§3 and 4.

2. Triple-deck theory for axisymmetric flows

Consider the high-Reynolds-number flow past a body of revolution at zero angle of attack in which there is a local disturbance in the vicinity of the streamwise station L_0^* due (say) to an abrupt surface-geometry change or an impinging external shock wave in the supersonic case. The consequent rapid change of the pressure and boundary-layer thickness causes a local interaction between the outside main stream and the laminar boundary-layer flow that takes place in a short region having the aforementioned lateral triple-deck structure of the disturbance field. Suppose that the fluid is Newtonian with constant Prandtl number and Chapman-Rubesin viscosity law and that the wall surface is maintained at a constant essentially adiabatic temperature. As shown in figure 1, we set up a local body-oriented coordinate system (x^*, y^*) with the origin centred in the interaction zone. The pressure, density, viscosity and temperature are denoted by p , ρ , μ and T ; u and v

are the velocity components in the x - and y -directions; the subscript ∞ refers to the conditions at the outer edge of the boundary layer in the absence of interaction, and the subscript w refers to the wall conditions. The superscript $*$ denotes the original dimensional physical variables, while scaled dimensionless variables will be denoted without an asterisk. L_0^* is the characteristic length which usually measures the distance of the interaction region from the nose of the body, r_0^* is the reference radius of the body corresponding to L_0^* , and r^* is the radial coordinate for a point in the flow field which is related to the (x^*, y^*) -coordinates by

$$r^* = r_0^* + y^* \cos \phi + x^* \sin \phi. \quad (1)$$

Here ϕ is the inclination of the body generator with respect to the symmetry axis. The same basic assumption as the two-dimensional version (Stewartson & Williams 1969; Stewartson 1971) is made that the interaction region consists of the three aforementioned decks, which is valid for all except very slender needle-like bodies.

For axisymmetric flow, the continuity equation in all three decks can be written in these coordinates as

$$\frac{\partial(r^*\rho^*u^*)}{\partial x^*} + \frac{\partial(r^*\rho^*v^*)}{\partial y^*} = 0. \quad (2)$$

The momentum equations are

$$\rho^*u^*\frac{\partial u^*}{\partial x^*} + \rho^*v^*\frac{\partial u^*}{\partial y^*} = -\frac{\partial p^*}{\partial x^*} + \frac{1}{r^*}\frac{\partial}{\partial y^*}\left(r^*\mu^*\frac{\partial u^*}{\partial y^*}\right), \quad (3)$$

$$\rho^*u^*\frac{\partial v^*}{\partial x^*} + \rho^*v^*\frac{\partial v^*}{\partial y^*} = -\frac{\partial p^*}{\partial y^*} + \dots \quad (4)$$

Here, for the middle deck and the upper deck, the viscous terms can be neglected, and, for the lower deck, only the viscous terms of the most importance are retained in the leading approximation. The energy equation for the upper and middle decks can be written as

$$\frac{1}{p^*}\frac{Dp^*}{Dt^*} - \frac{\gamma}{\rho^*}\frac{D\rho^*}{Dt^*} = 0 \quad (5)$$

for inviscid flows, where the substantial derivative is defined by

$$\frac{D}{Dt^*} = u^*\frac{\partial}{\partial x^*} + v^*\frac{\partial}{\partial y^*}$$

and γ is the ratio of specific heats. In the lower deck, the energy equation is not necessary because the flow velocity is so low that along an adiabatic wall incompressible disturbance flow occurs with fluid properties based on the wall temperature (Stewartson 1974).

From the general equations described above, we can see that the axisymmetric interaction problem differs from the two-dimensional one in the appearance of the radial coordinate r^* in the continuity equation for all three decks and in the momentum equation for the lower deck as a transverse curvature effect on the viscous term. Using (1), we note that we can rewrite (2) and (3) as

$$\frac{\partial(\rho^*u^*)}{\partial x^*} + \frac{\partial(\rho^*v^*)}{\partial y^*} + \rho^*u^*\frac{\sin \phi}{r^*} + \rho^*v^*\frac{\cos \phi}{r^*} = 0, \quad (6)$$

$$\rho^*u^*\frac{\partial u^*}{\partial x^*} + \rho^*v^*\frac{\partial u^*}{\partial y^*} = -\frac{\partial p^*}{\partial x^*} + \frac{\partial}{\partial y^*}\left(\mu^*\frac{\partial u^*}{\partial y^*}\right) + \mu^*\frac{\partial u^*}{\partial y^*}\frac{\cos \phi}{r^*}, \quad (7)$$

while (4) reduces to $dp^*/dy^* \approx 0$ for the thin inner deck.

The basic flow is assumed to be the undisturbed laminar boundary-layer flow on the body of revolution, which in general differs from a Blasius profile owing to the Mangler transformation (see below) except in the special case of a cylindrical body downstream of the nose. The local interaction with the main stream outside changes this velocity profile; in what follows, primed variables denote this perturbation field. Now a detailed analysis readily shows that the scaling law, the asymptotic analysis for $Re \rightarrow \infty$, and the matching steps are exactly the same as the two-dimensional version (see Stewartson 1974) and so will not be repeated here; thus it only remains to show when the explicit axisymmetry terms can be neglected and when they must be retained. It is known from the two-dimensional version that in all of the three decks the streamwise length scale has an order of ϵ^3 , where $\epsilon = Re^{-\frac{1}{2}}$ is a small parameter and $Re = \rho_\infty^* U_\infty^* L_0^* / \mu_\infty^*$, so that $x^* = O(\epsilon^3)$. We also have $p' = O(\epsilon^2)$.

Now we assume that we have a slender body $r_0^* = O(\epsilon^\beta)$ with $\beta > 0$ and that we are downstream of the stagnation region if it is not sharp-nosed such that

$$\cos \phi = O(1), \quad \sin \phi = O(\epsilon^\beta). \quad (8)$$

Since $y^* = O(\epsilon^4)$, $u' = O(\epsilon)$, $v' = O(\epsilon^2)$ and $\rho' = O(\epsilon)$ in the middle deck for either subsonic or supersonic external flow, we find that the first two terms of (6) are of order ϵ^{-2} , the third term of order unity, and the last term of order $\epsilon^{2-\beta}$. Thus, in the very-large-Reynolds-number limit, it can be seen that, if $\beta < 4$, the last two terms can be neglected in the leading approximation compared with the first two terms, reducing the equation to a two-dimensional form. Correspondingly, in the upper deck we have $y^* = O(\epsilon^3)$, $u' = O(\epsilon^2)$, $v' = O(\epsilon^2)$ and $\rho' = O(\epsilon^2)$; the same procedure shows that the first two terms in (6) are of order ϵ^{-1} , the third term is of order unity, and the last term is of order $\epsilon^{2-\beta}$. Thus, in the leading asymptotic $\epsilon \rightarrow 0$ approximation, the continuity equation here reduces to two-dimensional form if $\beta < 3$, whereas the axisymmetry terms must be retained when $\beta \geq 3$.

In the lower viscous-disturbance deck the appropriate scaled variables are $y^* = O(\epsilon^5)$, $u' = O(\epsilon)$, $v' = O(\epsilon^3)$ and $\rho^* = \rho_w^*$. It is then found that the first two terms in (6) are of order ϵ^{-2} , the third term of order ϵ , and the last term of order $\epsilon^{3-\beta}$. In the momentum equation (7) the two terms on the left-hand side are of order ϵ^{-1} , the second term on the right-hand side of order ϵ^{-1} , and the last term of order $\epsilon^{4-\beta}$. Therefore, the lower-deck equations also reduce to two-dimensional form when $\beta < 5$.

Summing up the above analysis of the leading approximation for $Re \rightarrow \infty$, the following general conclusions can be deduced for either subsonic or supersonic external flow. (i) The triple-deck equations for bodies of revolution with $r_0^* \sim \epsilon^\beta$ are exactly the same as those for two-dimensional flow when $\beta < 3$. In this case, the axisymmetric effect resides solely in the incoming undisturbed boundary-layer profile, as treated by the Mangler transformation (see §3.4). (ii) For the case $\beta = 3$, the flow in the upper deck is governed by the equation of axisymmetric potential flow, whereas in the middle and lower decks the flow is still governed by equations of two-dimensional form. (iii) For $\beta > 3$, the body of revolution is so slender that the middle deck will experience explicit three-dimensional effects that invalidate the aforementioned scaling laws. Furthermore, the boundary-layer thickness is comparable to the body thickness and thus is no longer described by the usual boundary-layer equations; instead, thick axisymmetric boundary-layer theory (White 1974, p. 347) must be applied. Fortunately this case is not of much practical interest and so will not be investigated further here.

Because of the already well-developed theory for two-dimensional triple-deck structure, we concentrate on the case $\beta = 3$ for a typical problem, to illustrate how

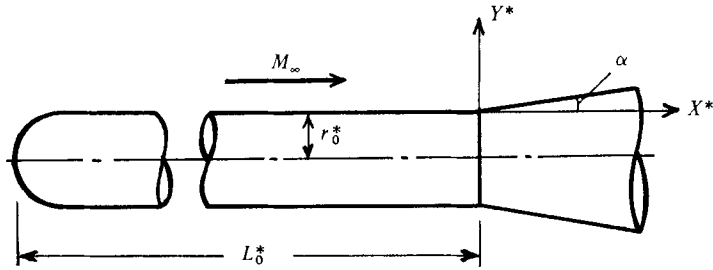


FIGURE 2. Flow past a cylindrical body with a conical frustum.

the explicit three-dimensional relief effects fundamentally alter viscous-inviscid interaction properties.

3. Compressive supersonic interaction in a flared body

3.1. Mathematical formulation

As shown in figure 2, we consider compressible flow past a cylindrical body of revolution followed by a conical frustum or flare where a compressive boundary-layer interaction takes place at the corner. Let α denote the flare angle; the body radius is supposed to be of order ϵ^3 .

The Blasius solution can be assumed for the undisturbed boundary-layer flow on the cylindrical part of the body, since this flow is the same as that on a flat plate in the absence of transverse curvature effects. As demonstrated in the last section, the present problem differs from the two-dimensional version only in the upper deck where we have axisymmetric potential flow. Thus we may introduce the two-dimensional lower-deck scaling (Stewartson 1974):

$$\left. \begin{aligned} x^* &= \epsilon^3 a x, & a &= L_0^* C^{\frac{3}{8}} \lambda^{-\frac{3}{4}} \delta^{-\frac{3}{8}} \left(\frac{T_w^*}{T_\infty^*} \right)^{\frac{3}{2}}, \\ y^* &= \epsilon^5 b y, & b &= L_0^* C^{\frac{3}{8}} \lambda^{-\frac{3}{4}} \delta^{-\frac{1}{8}} \left(\frac{T_w^*}{T_\infty^*} \right)^{\frac{3}{2}}, \\ p^* &= p_\infty^* + \epsilon^2 c p, & c &= \rho_\infty^* U_\infty^{*2} C^{\frac{1}{4}} \lambda^{\frac{1}{2}} \delta^{-\frac{1}{4}}, \\ u^* &= \frac{\epsilon d}{b} u, & d &= L_0^* U_\infty^* C^{\frac{3}{4}} \lambda^{-\frac{1}{2}} \delta^{-\frac{1}{4}} \left(\frac{T_w^*}{T_\infty^*} \right)^2, \\ v^* &= \frac{\epsilon^3 d}{a} v, & \alpha^* &= \epsilon^2 \frac{b}{a} \alpha, \end{aligned} \right\} \quad (9)$$

where $C \equiv \mu_w^* T_\infty^* / \mu_\infty^* T_w^*$, $\delta \equiv |M_\infty^2 - 1|$, and λ is a value determined by the slope of the velocity profile at the wall in the basic undisturbed boundary layer (for the present example $\lambda = 0.3321$). The resulting problem then reduces to solving the inner-deck equations

$$\begin{aligned} \frac{\partial u}{\partial x} + \frac{\partial v}{\partial y} &= 0, \\ u \frac{\partial u}{\partial x} + v \frac{\partial u}{\partial y} &= -\frac{dp}{dx} + \frac{\partial^2 u}{\partial y^2} \end{aligned} \quad (10)$$

with the no-slip impermeable wall boundary conditions

$$u = v = 0 \quad \text{at} \quad y = \alpha H(x) x \quad (11)$$

plus the inner-outer matching condition (see Stewartson 1974)

$$u \rightarrow y + A(x) \quad \text{as} \quad y \rightarrow \infty. \quad (12)$$

Here $H(x)$ is Heaviside's unit function and $-A(x)$ can be regarded as a displacement thickness which is transmitted unchanged through the middle deck to the upper deck and linked with the pressure distribution by the solution to the linearized potential-flow equation in the upper deck.

Now let us restrict attention to the case of supersonic flow $M_\infty > 1$, where the flare-generated compression takes place across an oblique shock. In the region very close to the corner where the radius of the body has only a little change, a quasicylindrical approximation can be applied to relate p to A as follows (see Ward 1955, p. 169):

$$p(x) = - \left\{ A'(x) - \frac{1}{r_0} \int_{-\infty}^{\infty} W \left(\frac{x-s}{r_0} \right) A'(s) ds \right\}, \quad (13)$$

where $A(-\infty) = 0$, $W(z)$ is a function which has been given in figure 8.1 of Ward (1955), and where the upper limit of the integration has been replaced by ∞ because $W(z) = 0$ for $z < 0$. Here the scaled radius of the body is defined by

$$r_0 \equiv \frac{\delta^{1/2} r_0^*}{a \epsilon^3} \sim \frac{\delta^{1/2} \epsilon^2}{a \epsilon^3} \sim \frac{\delta^{1/2}}{a} = O(1). \quad (14)$$

We note that $W(z)$ has the closed-form Laplace transform

$$\int_0^\infty W(z) e^{-sz} dz = \frac{K_1(s) - K_0(s)}{K_0(s)}, \quad (15)$$

where K_0 and K_1 are modified Bessel functions. The resulting problem is thus closed by (10)–(13), but the solution to these nonlinear equations in general must be obtained numerically.† However, under the assumption that the flare angle α is sufficiently small, an instructive linearized solution can be obtained in closed analytical form as presented in §3.2.

3.2. *Linearized approximation*

We consider weak compressive interactions due to small flare angles; to a first approximation, following Stewartson (1971), we thus take

$$\left. \begin{aligned} u(x, y) &= y + \alpha U(x, y), \\ v(x, y) &= \alpha V(x, y), \\ p(x) &= \alpha P(x), \end{aligned} \right\} \quad (16)$$

where U , V and P are the disturbance-amplitude distribution functions. Then substituting into (10), linearizing the results to first order in α and then taking the Fourier transform with respect to x , the closed-form solution of the resulting well-known ordinary differential equation for \bar{U} that dies out at infinity is easily obtained as

$$\frac{\partial \bar{U}}{\partial y} = C(k) \text{Ai} [(0 + ik)^{1/3} y], \quad (17)$$

† An efficient iterative method based on the Fourier transform, for example, is described by Duck (1983).

where

$$\bar{U}(y, k) = \int_{-\infty}^{\infty} U(x, y) e^{-ikx} dx$$

denotes the Fourier transform. Here Ai denotes the Airy function of argument $(0 + ik)^{\frac{1}{3}}$, assumed to be regular in the k -plane cut along the positive imaginary axis. The constant $C(k)$ here can be determined by integrating (17) with respect to y , using known integral properties of the Airy function, and then applying the transform of the linearized version of conditions (11) and (12).

The corresponding pressure distribution transform can now be found by using the so-called compatibility condition obtained by satisfying the momentum equation (10) at the wall; from its transform in the linear approximation, this yields

$$\bar{P}(k) = \frac{\theta^{\frac{1}{3}}}{ikN(k)}, \tag{18}$$

where

$$\left. \begin{aligned} \theta &\equiv [-3 \text{Ai}'(0)]^{\frac{1}{3}} = 0.8272, \\ N(k) &\equiv \theta^{\frac{1}{3}} T(ir_0 k) - (0 - ik)^{\frac{1}{3}}, \\ T(z) &\equiv \frac{K_0(z)}{2K_0(z) - K_1(z)}. \end{aligned} \right\} \tag{19}$$

The inversion of (18) can be carried out by the Faltung theorem to obtain

$$P(x) = \int_{-\infty}^x (x - \xi) Q(\xi) d\xi, \tag{20}$$

where

$$Q(\xi) = \frac{1}{2\pi} \int_{-\infty}^{\infty} \bar{Q}(k) e^{ik\xi} dk, \tag{21}$$

$$\bar{Q}(k) = \frac{\theta^{\frac{1}{3}} ik}{N(k)}. \tag{22}$$

For $\xi < 0$, the integration path along the entire real axis can be closed by a half-circle of infinite radius in the lower plane. Since it can be shown that the function $N(k)$ has a zero $k = -i\kappa_1$ on the negative imaginary axis (where κ_1 can be found by numerical procedure), the residue theorem yields

$$Q(\xi) = \frac{\kappa_1 \theta^{\frac{1}{3}} e^{\kappa_1 \xi}}{iN'(-i\kappa_1)} \quad (\xi < 0), \tag{23}$$

where, in terms of the Bessel functions K_0 and K_1 ,

$$iN'(-i\kappa_1) = \frac{\theta^{\frac{1}{3}} \{ K_1(r_0 \kappa_1) K_0(r_0 \kappa_1) + r_0 \kappa_1 [K_0^2(r_0 \kappa_1) - K_1^2(r_0 \kappa_1)] \}}{[2K_0(r_0 \kappa_1) - K_1(r_0 \kappa_1)]^2} + \frac{4}{3} \left(\frac{\kappa_1}{\theta} \right)^{\frac{1}{3}}. \tag{24}$$

Using (23) and (24), the integration of (20) can be carried out to yield

$$P(x) = \frac{1}{\kappa_1^2} Q(x) \quad (x < 0). \tag{25}$$

We note here that, in the limiting case $r_0 \rightarrow \infty$, it can be shown that $T(ir_0 k) \rightarrow 1$, which from (19) gives for the zero of $N(k)$ the closed result $\kappa_1 = \theta$. Correspondingly one finds that

$$P(x) \rightarrow \frac{2}{3} e^{\theta x} \quad \text{as } r_0 \rightarrow \infty, \tag{26}$$

which is exactly the two-dimensional result given by Stewartson (1971).

Turning to the downstream region $\xi > 0$, it may be expected that the integrand

in (21) is regular in the upper half of the plane cut along the positive imaginary axis, so that the $Q(\xi)$ integration along the entire real axis can be changed into that around the positive imaginary axis. After some algebraic manipulation, the result is

$$Q(\xi) = \frac{\theta^2}{\pi} \int_0^\infty \text{Im} \left\{ \frac{T(e^{\pi i} r_0 \eta \theta)}{\eta} + e^{\frac{1}{2} \pi i} \eta^{\frac{1}{2}} \right\}^{-1} e^{-\eta \theta \xi} d\eta \quad (\xi > 0). \tag{27}$$

Equation (20) then yields

$$\begin{aligned} P(x) &= \int_{-\infty}^0 (x - \xi) Q(\xi) d\xi + \int_0^x (x - \xi) Q(\xi) dx \\ &= (1 + \kappa_1 x) P(-0) \\ &\quad + \frac{\theta^2}{\pi} \int_0^\infty \frac{e^{-\eta \theta x} - 1 + \eta \theta x}{(\eta \theta)^2} \text{Im} \left\{ \frac{T(e^{\pi i} r_0 \eta \theta)}{\eta} + e^{\frac{1}{2} \pi i} \eta^{\frac{1}{2}} \right\}^{-1} d\eta \quad (x > 0), \end{aligned} \tag{28}$$

where Im denotes the imaginary part. The indicated integration can be carried out numerically with care as shown in the appendix.

With the pressure field in hand, the scaled perturbation shear stress may now be determined as

$$\tau = \left(\frac{\partial u}{\partial y} \right)_{y=0} = 1 + \alpha \left(\frac{\partial U}{\partial y} \right)_{y=0}. \tag{29}$$

From the foregoing solution we have

$$\left(\frac{\partial U}{\partial y} \right)_{y=0} = \frac{\text{Ai}(0)}{\text{Ai}'(0)} (0 + ik)^{\frac{2}{3}} \bar{P}(k), \tag{30}$$

so that substituting (18) and inverting by use of the Faltung theorem yields

$$\left(\frac{\partial U}{\partial y} \right)_{y=0} = \int_{-\infty}^\infty H(x - \xi) Z(\xi) d\xi = \int_{-\infty}^x Z(\xi) d\xi, \tag{31}$$

where

$$Z(\xi) = \frac{1}{2\pi} \frac{\text{Ai}(0)}{\text{Ai}'(0)} \int_{-\infty}^\infty \frac{\theta^{\frac{2}{3}} e^{ik\xi} dk}{(0 + ik)^{\frac{2}{3}} \left[\theta^{\frac{1}{3}} \frac{T(ir_0 k)}{ik} - (0 + ik)^{\frac{1}{3}} \right]}. \tag{32}$$

Applying the residue theorem leads to the final results that

$$\left(\frac{\partial U}{\partial y} \right)_{y=0} = \left\{ \begin{aligned} &-3 \frac{\text{Ai}(0)}{\theta^{\frac{2}{3}}} \kappa_1^{\frac{2}{3}} P(x) \quad (x < 0), \\ &\left(\frac{\partial U}{\partial y} \right)_{y=0} + \frac{3 \text{Ai}(0)}{\pi \theta^{\frac{2}{3}}} \int_0^\infty \frac{1 - e^{-\eta \theta x}}{\eta^{\frac{2}{3}}} \text{Re} \left\{ \frac{e^{\frac{1}{2} \pi i}}{\frac{T(e^{\pi i} r_0 \eta \theta)}{\eta} + e^{\frac{1}{2} \pi i} \eta^{\frac{1}{2}}} \right\} d\eta \end{aligned} \right\} \quad (x > 0), \tag{33}$$

where Re denotes the real part. The indicated integration again can be carried out numerically as shown in the appendix.

3.3. Discussion of results

The upstream influence is determined by the zero of the function $N(-i\kappa)$; figure 3 shows this function plotted versus κ for a typical r_0 , from which we see that a zero κ_1 exists for $r_0 \kappa > 0.381$. Figure 4 presents the calculated κ_1 as a function of $1/r_0$, which is nearly a linear function. It is seen that the two-dimensional result $\kappa_1 = 0.8272$

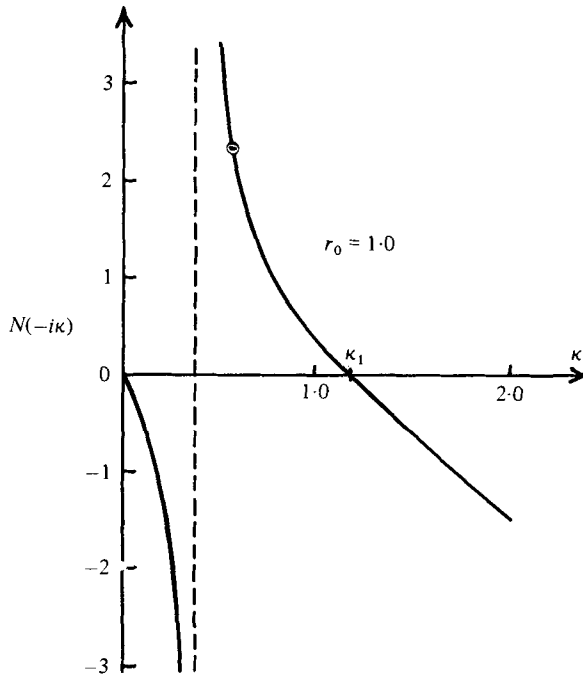


FIGURE 3. $N(-i\kappa)$ as a function of κ for $r_0 = 1$.

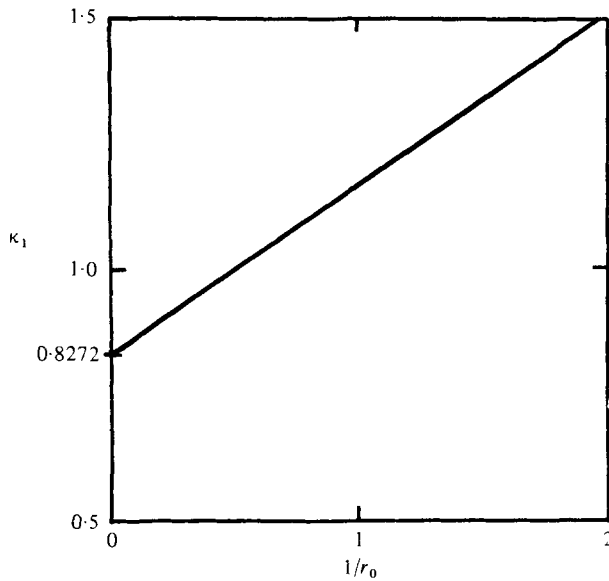


FIGURE 4. The zero of the function $N(-i\kappa)$ versus $1/r_0$.

is approached in the limit $r_0 \rightarrow \infty$, and that κ_1 increases as r_0 decreases. Because κ_1 is the logarithmic decrement introduced by Lighthill (1953), this result implies that the upstream influence distance of the disturbance from the conical frustum decreases with an increasing three-dimensional relief effect.

The pressure and shear-stress distributions calculated from (25), (28) and (33) are

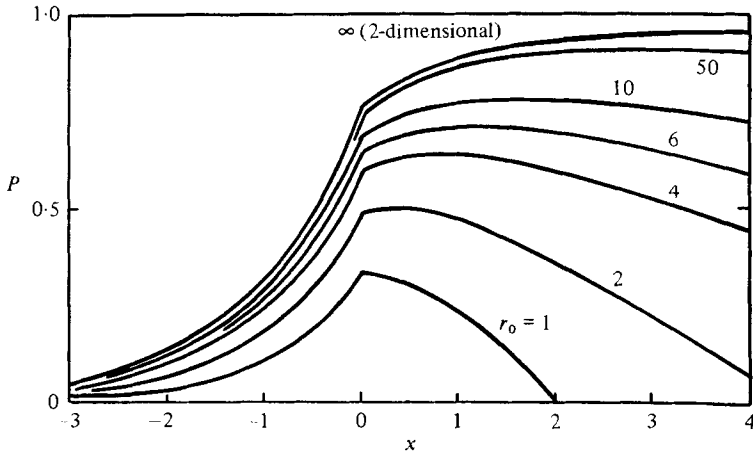


FIGURE 5. Pressure distribution.

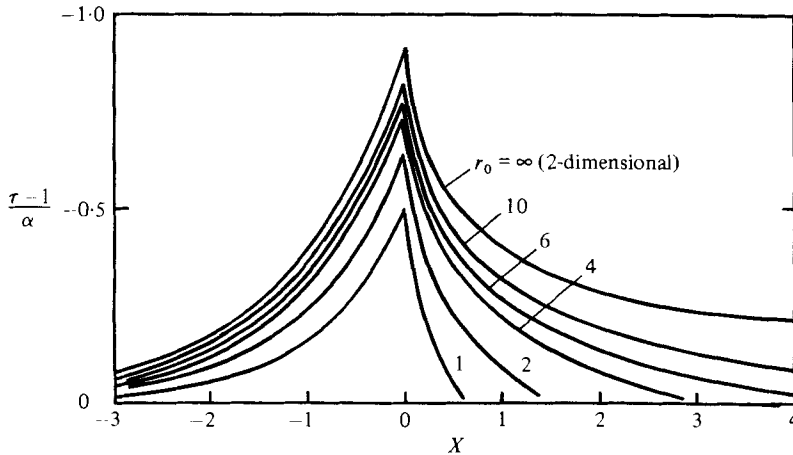


FIGURE 6. Disturbed shear-stress distribution.

plotted in figures 5 and 6 for different r_0 . These curves in the $r_0 = \infty$ limit correspond to the two-dimensional solution studied by Stewartson (1971); with decreasing r_0 it is seen that the interactive disturbance decreases owing to the three-dimensional relief effects. It may be noted in this connection that a closed-form solution can be obtained in the formal limit $r_0 \rightarrow 0$ that yields zero upstream disturbance for $x < 0$ and negative pressure perturbation downstream for $x > 0$; however, this mathematical limit has no physical meaning in the present study because of the abovementioned exclusion of transverse curvature effects that would, in fact, actually be important in such a limit. For comparison figure 7 illustrates results based on the linearized potential-flow theory; it shows that the cylindrical part of the body experiences no disturbance from the corner because the perturbation cannot travel upstream in inviscid supersonic flow, and that two-dimensional compression occurs at the corner, followed by a pressure decay to the value for a cone (exact theory) or to a value of zero (quasicylindrical approximation). Since the present theory shows that the initial pressure rise due to the flow deflection is lower than the two-dimensional value when viscous interaction effects are included, the pressure decay along the flare is even more rapid and yields negative values far downstream as a result of the quasicylindrical-

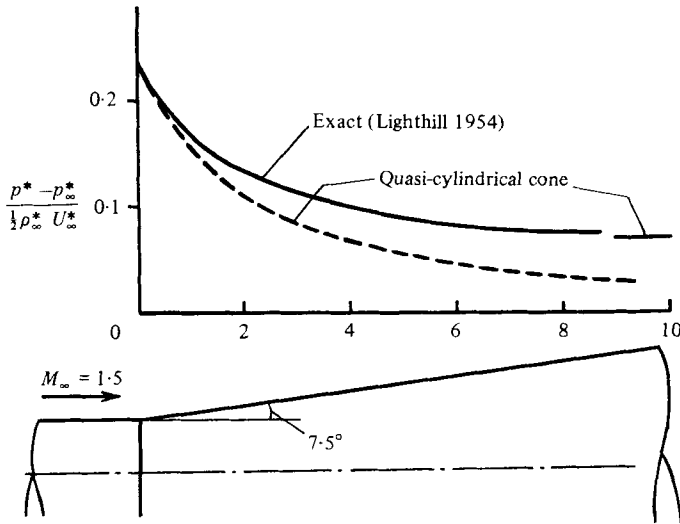


FIGURE 7. Pressure distribution by potential-flow theories.

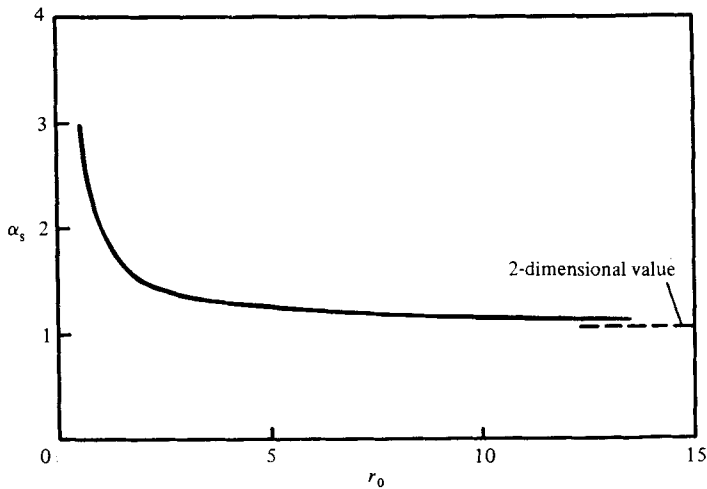


FIGURE 8. Flow deflecting angle for provoking separation.

flow approximation used on the flare; this could be readily corrected by using instead a locally conical ('tangent-cone') flow model downstream.

The disturbance skin-friction results also enable an estimate of when incipient flow separation occurs near the corner, an event of both basic and practical interest. To be sure, separation itself is not accurately predicted by the present linear approximation because it implies that the disturbed shear stress is much smaller than the Blasius one; nevertheless, it does give a rough indication of when separation ($\tau' + \tau_0 \approx 0$) is imminent. Figure 6 shows that the minimum shear stress occurs at the corner, so that flow separation will occur there when α is sufficiently large. The lowest value of the flare angle α_s at which separation occurs is

$$\alpha_s = -1 / \left(\frac{\partial U}{\partial y} \right)_{y=0, x=0} ;$$

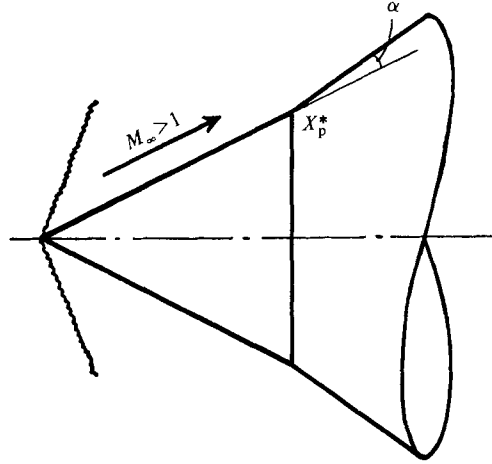


FIGURE 9. Supersonic flow past a double cone.

figure 8 presents the results of the linear-theory prediction for α_s as a function of r_0 ; as expected, α_s increases owing to the three-dimensional relief effects.

3.4. The role of an inclined forebody

According to the general triple-deck theory in §2, the presence of a non-cylindrical forebody would modify the foregoing results by virtue of its influence on the undisturbed incoming boundary layer via the Mangler transformation (indeed, for $\beta < 3$, this influence would be the *only* three-dimensional effect: the above results would be negligible in the leading asymptotic approximation). For example, consider a supersonic flow past a flared cone as shown in figure 9, where the forecone region is the basic undisturbed flow. Then by the Mangler transformation, the flow around the forecone can be transformed into a flow past a flat plate; thus for the cone, the key property at the undisturbed boundary-layer velocity profile at the wall on which the interaction depends is

$$\left(\frac{dU_0}{dy^*}\right)_{y^*=0} = \sqrt{3} \lambda \frac{T_\infty^* U_\infty^*}{T_w^* x_p^*} \left(\frac{\rho_\infty^* U_\infty^* x_p^*}{\mu_\infty^*}\right)^{\frac{1}{2}} C^{-\frac{1}{2}}, \quad (34)$$

where x_p^* is the distance measured along the cone generator from the nose to the corner and $\lambda = 0.3321$ is the Blasius-solution value. In comparison with the two-dimensional version, this expression differs from the flat-plate result only in the factor $\sqrt{3}$: thus, for the present example, we need only use $\lambda = 0.3321\sqrt{3}$ in (9) instead of 0.3321 in two-dimensional flow. This immediately implies that the perturbation from the flare has an even smaller upstream influence than that due to a two-dimensional flap at the same angle predicted above, because of the higher velocity near the wall in the boundary layer on the body of revolution.

4. Concluding remarks

Owing to the restrictions imposed by the very large Reynolds number limit of the present theory, direct detailed quantitative comparisons of our results with available experiment are difficult (see e.g. Burggraf 1975). Nevertheless, support for the

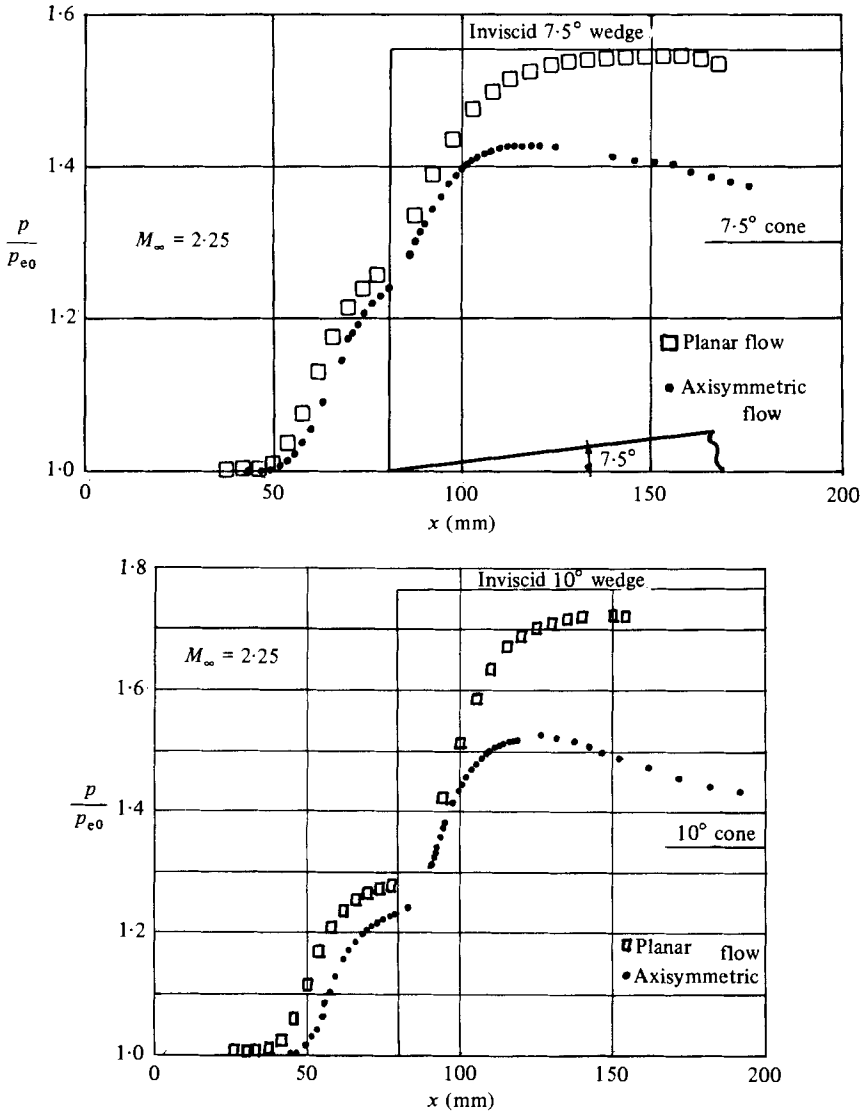


FIGURE 10. Two-dimensional versus axisymmetric flare interaction pressure distributions: experiments of Ginoux (1969).

qualitative predictions of the axisymmetric three-dimensional effects on local viscous-inviscid interaction can be found in several experimental studies of laminar boundary-layer-compression-corner interactions. For example, Kuehn's (1962) experiments have shown that the upstream influence distance of a flare-induced supersonic laminar interaction on a cylinder is indeed smaller than that due to a two-dimensional ramp of the same angle, while incipient separation occurs at a noticeably higher deflection angle as our analysis suggests. The data obtained by Ginoux (1969) at Mach 2.25, illustrated here in figure 10, in terms of the comparative interactive pressure distributions on a wedge versus flare for two different deflection angles, also strongly support the theoretical predictions shown in figure 5: the axisymmetric flare clearly

causes a shorter and lower-level interactive influence region than the flap of the same angle. Similar experimental results at higher Mach numbers have also been presented by Stollery (1975).

Appendix. Numerical treatment of certain integrals in the theory

In the evaluation of the integral in (28), the function $T(e^{\pi i} r_0 \eta \theta)$ is evaluated by using the following expressions deduced from equation (6.9.31) of Abramowitz & Stegun (1965):

$$K_0(e^{\pi i} r_0 \eta \theta) = K_0(r_0 \theta \eta) - \pi i I_0(r_0 \theta \eta),$$

$$K_1(e^{\pi i} r_0 \eta \theta) = -K_1(r_0 \theta \eta) - \pi i I_1(r_0 \theta \eta),$$

where I_0 and I_1 are modified Bessel functions. Moreover, great care must be taken in the subsequent numerical quadrature because of its slow convergence as $\eta \rightarrow \infty$. It can be shown that the integrand goes to zero as $\eta \rightarrow 0$ and behaves as $-\sqrt{3}x/2\theta\eta^{\frac{3}{2}}$ for $\eta \rightarrow \infty$, so that the integral is carried out first from 0 to the limit of some large given value B (say) by Simpson's rule, then from B to ∞ by the analytical result

$$-\frac{\sqrt{3}x}{2\theta} \int_B^\infty \frac{d\eta}{\eta^{\frac{3}{2}}} = -\frac{3\sqrt{3}x}{2\theta B^{\frac{3}{2}}},$$

which gives a non-trivial contribution to the total value of the integral even for a very large value of B .

Turning to the integral in (33), even more care is required in its numerical evaluation, not only because of slow convergence as $\eta \rightarrow \infty$ but also because of special handling of its lower limit $\eta \rightarrow 0$. The integrand behaves as $\eta^{-\frac{1}{2}}/\log(\frac{1}{2}r_0\theta\eta)$ for $\eta \rightarrow 0$, and as $1/\eta^{\frac{3}{2}}$ for $\eta \rightarrow \infty$, so that the entire interval of the integration is divided into three parts: from 0 to A , from A to B , and B to ∞ , where A and B are suitably small and large values respectively. Then the integral on the first interval is found by the approximation

$$\int_0^A \frac{dx}{x^{\frac{3}{2}} \log x} = \int_{-\infty}^{\log A} \frac{e^{\frac{3}{2}y}}{y} dy$$

with the use of numerical quadrature, the second interval is treated by Simpson's rule, and the last by the analytical result

$$\int_B^\infty \frac{d\eta}{\eta^{\frac{3}{2}}} = \frac{2}{3} B^{-\frac{3}{2}}.$$

REFERENCES

- ABRAMOWITZ, M. & STEGUN, I. A. 1965 *Handbook of Mathematical Functions*. National Bureau of Standards.
- BURGGRAF, O. 1975 Asymptotic theory of separation and reattachment of a laminar boundary layer on a compression ramp. *AGARD. CP-168 on Flow Separation*, pp. 10-1-10-9.
- DAVIS, R. T. & WERLE, M. J. 1976 Numerical methods for interacting boundary layers. In *Proc. Heat Transfer Fluid Mech. Inst.*, pp. 317-339. Stanford University Press.
- DUCK, P. W. 1981 Laminar flow over a small unsteady three-dimensional hump. *Z. angew. Math. Phys.* **32**, 62-79.
- DUCK, P. W. 1983 The effect of a surface discontinuity on an axisymmetric boundary layer. *Q. J. Math. Appl. Mech.* (To be published.)
- GINOUX, J. 1969 High speed flows over wedges and flares with emphasis on a method of detecting transition. In *Viscous Interaction Phenomena in Supersonic and Hypersonic Flows*, pp. 523-538. University of Dayton Press.

- INGER, G. R. 1980 Upstream influence and skin friction in non-separating shock-turbulent boundary layer interactions. *A.I.A.A. Paper* 80-1411.
- JENSON, R., BURGGRAF, O. & RIZZETTA, D. 1975 Asymptotic solution for supersonic viscous flow past a compression corner. In *Proc. 4th Int. Conf. on Num. Meth. Fluid Dyn.* (ed. R. D. Richtmyer). Lecture Notes in Physics, vol. 35. Springer.
- KUEHN, D. M. 1962 Laminar boundary layer separation induced by flares on cylinders at zero angle of attack. *NASA. Tech. Rep.* R-146.
- LIGHTHILL, M. J. 1953 On boundary layers and upstream influence. II. Supersonic flows without separation. *Proc. R. Soc. Lond. A* **217**, 478-507.
- LIGHTHILL, M. J. 1954 Higher approximations. In *General Theory of High Speed Aerodynamics*, vol. VI, §E. Princeton University Press.
- MESSITER, A. F. 1970 Boundary layer flow near the trailing edge of a flat plate. *SIAM. J. Appl. Math.* **18**, 241-247.
- NEILAND, V. YA. 1969 Contribution to a theory of separation of a laminar boundary layer in supersonic stream. *Izv. Akad. Nauk SSSR., Mekh. Zhid. i Gaza* **4**, 53-57 (in Russian).
- RYZHOV, O. S. 1980 Unsteady three-dimensional boundary layer, freely interacting with an outer stream. *Prik. Mat. Mekh.* **44**, 1035-1052 (in Russian).
- SMITH, F. T. 1973 Laminar flow over a small hump on a flat plate. *J. Fluid Mech.* **57**, 803-829.
- SMITH, F. T., SYKES, R. I. & BRIGHTON, P. W. M. 1977 A two-dimensional boundary layer encountering a three-dimensional hump. *J. Fluid. Mech.* **83**, 163-176.
- STEWARTSON, K. 1971 On laminar boundary layers near corners. *Q. J. Mech. Appl. Math.* **23**, 137-152 [Corrections and addition. **24**, 387-389].
- STEWARTSON, K. 1974 Multistructured boundary layers on plates and related bodies. *Adv. Appl. Mech.* **14**, 146-239.
- STEWARTSON, K. & WILLIAMS, P. G. 1969 Self-induced separation. *Proc. R. Soc. Lond. A* **313**, 181-206.
- STOLLERY, J. L. 1975 Laminar and turbulent boundary layer separation at supersonic and hypersonic speeds. *AGARD. CP-168 on Flow Separation*, pp. 20-1-20-10.
- TU, K. M. & WEINBAUM, S. 1976 A non-asymptotic triple-deck model for supersonic boundary layer interaction. *A.I.A.A. J.* **14**, 767-775.
- WARD, G. N. 1955 *Linearized Theory of Steady High-Speed Flow*. Cambridge University Press.
- WHITE, F. M. 1974 *Viscous Fluid Flow*. McGraw-Hill.
- WILLIAMS, P. G. 1975 A reverse flow computation in the theory of self-induced separation. In *Proc. 4th Int. Conf. Num. Meth. Fluid Dyn.* (ed. R. D. Richtmyer). Lecture Notes in Physics, vol. 35. Springer.